Biochimica et Biophysica Acta, 734 (1983) 295–308
Elsevier

BBA 71845

PHASE FLUOROMETRIC STUDIES OF SPECTRAL RELAXATION AT THE LIPID-WATER INTERFACE OF PHOSPHOLIPID VESICLES

JOSEPH R. LAKOWICZ, RICHARD B. THOMPSON and HENRYK CHEREK

University of Maryland, School of Medicine, Department of Biological Chemistry, Baltimore, MD 21201 (U.S.A.)

(Received February 21st, 1983)
(Revised manuscript received June 20th, 1983)

Key words: Lipid/water interface; Fluorescence; Phase behavior; Phospholipid; (Model membrane)

We examined the dynamic properties of the lipid-water interface region of model membranes using the probe 2-*p*-toluidinylnaphthalene-6-sulfonic acid (TNS). For comparison we also examined the temperature-dependent spectral properties of TNS in the viscous solvent glycerol. Fluorescence phase shift and demodulation measurements were used to prove that the membranes relax around the excited state of TNS on the ns time scale. The rate of spectral relaxation is thought to reflect the mobility of the polar interface region of the membranes on this same time scale. The spectral relaxation times were estimated by the use of phase-sensitive detection of fluorescence. Using this method one may directly record, in an approximate fashion, the emission spectra of the relaxed and the initially excited states of TNS. The relative intensities of these phase-sensitive spectra, in combination with the measured phase and modulation values on the short and long wavelength sides of the emission, yield the spectral relaxation times. For saturated and unsaturated phosphatidylcholines, at temperatures ranging from 5 to 50°C, the relaxation times ranged from 5 to 1 ns. The activation energies for spectral relaxation were near 4 kcal/mol. Surprisingly, the relaxation times decreased smoothly with increasing temperature, and did not change abruptly at the phase transition temperatures. These results indicate that the small molecular motions of the interface region of membranes, which are responsible for spectral relaxation, are not dramatically influenced by the phase state of the acyl side chain region of the membranes.

Introduction

The functional properties of cell membranes appear to be dependent upon the dynamic properties of the lipid molecules which compose the bilayers [1–2]. For example, the activity of membrane-bound proteins, the passive permeabilities of membranes to ions and the adaptation of organisms to temperature all appear to be dependent upon the chemical composition and temperature-dependent phase behavior of the membranes. To explain these phenomena the effects of phospholipid composition and temperature on membranes have been widely studied using a number of physical methods. Among these methods fluorescence spectroscopy has been particularly useful because of its high inherent sensitivity, its natural time window in the ns range, and the ease with which non-polar fluorophores can be incorporated into both model and natural membranes. Such probes typically localize in the acyl side chain region of the membranes. Consequently, it is this region which has been most widely studied, as is typified by the analysis of phase transitions and

Abbreviations: TNS, 2-*p*-toluidinylnaphthalene-6-sulfonic acid; DOPC, DMPC and DPPC, dioleoyl-, dimyristoyl-, and dipalmitoyl-L-α-phosphatidylcholine, respectively.

order parameters using the probe 1,6-diphenylhexatriene [3–6]. These studies revealed a dramatic change in the apparent microviscosities and/or order parameters of the membranes at the phase transition temperatures.

We chose to study a different dynamic property of the membranes, this being the ability of polar headgroups of the lipids to reorient or relax around the increased dipole moment of a fluorophore in the excited state. Such motions are the origin of time-dependent spectral shifts to longer wavelengths. The rate of these shifts reflects the rate of motion of polar groups surrounding the fluorophore. We will refer to this phenomenon as solvent or dipolar relaxation, even when the fluorophore is bound to the membranes. As an example of this phenomenon we recall the well-known blue shift of fluorescence emission spectra at low temperatures. Such shifts occur because, at lower temperatures, the solvent relaxation time becomes longer than the fluorescence lifetime. Consequently, emission from the unrelaxed state is observed. At higher temperatures, relaxation is complete prior to emission, and the relaxed red-shifted emission is observed. A more detailed description of solvent relaxation has been presented elsewhere [7,8]. Frequently, for fluorophores which are bound to macromolecules, the rate of solvent relaxation is comparable to the rate of fluorescence emission [9,10]. Then, following pulsed excitation, the emission spectrum displays time-dependent spectral shifts to lower energies or longer wavelengths.

TNS is a fluorophore which is sensitive to solvent polarity and which localizes at the lipid-water interface region of membranes [11–13]. Previously, time-resolved emission spectra of TNS-labeled membranes were used to determine the spectral relaxation rates [9,10]. In contrast to the earlier time-resolved studies of spectral relaxation we used the techniques of phase-modulation fluorometry and phase-sensitive detection of fluorescence [14,15]. Using the former method we show that time-dependent processes, and not spectral heterogeneity, are the origin of the wavelength-dependent fluorescence decays of TNS-labeled membranes. Then we used phase-sensitive detection of fluorescence to directly record the emission spectra of the relaxed and the unrelaxed states [19]. Using these data the spectral relaxation times may be calculated.

Theory

Effects of an excited state reaction on fluorescence phase and modulation values

The phenomenon of solvent relaxation is a complex process which involves a number of solvent-fluorophore interactions [16]. Solvent relaxation may be described using a continuous relaxation model, as described by Bakhshiev et al. [17], using multiple-step models [18], or most simply using a two-state model [19]. The latter model is advantageous, and will be used in our analysis, because of its simple theoretical formalism and the ease with which the experimental data can be used to determine the spectral relaxation time τ_s. Furthermore, for modest spectral shifts, such as those shown by TNS, this simple model provides a good approximation of the wavelength-dependent phase and modulation data [20,21].

In the two-state model it is assumed that upon excitation the fluorophore is in an initially excited state (F). This state can be decay either by return to the ground state with a rate constant Γ, or by relaxation to a red-shifted or relaxed state (R) with a rate constant k. For simplicity it is assumed that relaxation is irreversible. We also assume that relaxation does not affect the decay rate of the fluorophore. Hence, if the R-state could be excited directly, its decay rate would also be Γ. The lifetime of the F-state is given by $\tau_F = (\Gamma + k)^{-1}$, and the lifetime which is unaffected by relaxation is $\tau_0 = \Gamma^{-1}$. The decay of the R-state is doubly exponential. The relative quantum yields of the F and R states are given by

$$\alpha_F = \frac{\Gamma}{\Gamma + k} \tag{1}$$

$$\alpha_R = \frac{k}{\Gamma + k} \tag{2}$$

This model has been solved previously for the case of sinusoidally modulated excitation [19,20]. The total intensity at any wavelength λ is given by

$$I(\lambda, t) = \alpha_F m_F I_F^0(\lambda) \sin(\omega t - \phi_F) + \alpha_R m_R I_R^0(\lambda) \sin(\omega t - \phi_R) \tag{3}$$

where ω is the circular modulation frequency, ϕ_i are the phase angles of the F and R states, $I_i^0(\lambda)$

are the emission spectra normalized to unit area and m_i are the modulations of the emission of each state relative to the modulation of the incident light. The phase angles are given by

$$\tan \phi_F = \omega/(\Gamma + k) = \omega\tau_F \tag{4}$$

$$\tan \phi_R = \frac{\omega(2\Gamma + k)}{\Gamma(\Gamma + k) - \omega^2} \tag{5}$$

and the demodulation factors are

$$m_F = \frac{\Gamma + k}{\sqrt{(\Gamma + k)^2 + \omega^2}} \tag{6}$$

$$m_R = m_F \frac{\Gamma}{\sqrt{\Gamma^2 + \omega^2}} \tag{7}$$

Since relaxation is accompanied by a spectral shift, one expects that these values of ϕ_i and m_i will be observed on the blue and red sides of the emission. This is in fact observed for excited state processes in which the spectral shifts are large [21]. However, in many cases, including the TNS-labeled membranes described in this report, there is significant spectral overlap of the emission from the F and R states even at the extreme edges of the emission spectra. The measured values of ϕ and m are then a weighted average of those expected for the F and R states, with the F-state emission being dominant at short wavelengths and the R-state emission being dominant at longer wavelengths.

Conveniently, the measured phase and modulation values allow time-dependent spectral shifts to be distinguished from ground state heterogeneity; that is, a mixture of fluorophore populations with different lifetimes. The possibility of distinguishing an excited process from heterogeneity arises from the additive property of the individual phase angles and the multiplicative property of the demodulation factors (Eqn. 6). Let ϕ_0 be the phase angle in the absence of relaxation, $\tan \phi_0 = \omega\tau_0$. Then, using the law for the tangent of a sum one finds that

$$\phi_R = \phi_F + \phi_0. \tag{8}$$

The phase angle of the R-state, relative to the excitation, is the sum of the phase angles of the F-state and that expected for the R-state, if the latter could be directly excited (ϕ_0). Recalling that $m_i = \cos \phi_i$ [20,22] combination of Eqns. 6, 7 and 8 yields

$$\frac{m_R}{\cos \phi_R} = \frac{\cos \phi_0 \cos \phi_F}{\cos(\phi_0 + \phi_F)} \tag{9}$$

Using the law for the cosine of a sum, followed by division by $\cos \phi_0 \cos \phi_F$, yields

$$\frac{m_R}{\cos \phi_R} = \frac{1}{1 - \tan \phi_0 \tan \phi_F} = \frac{1}{1 - \omega^2 \tau_0 \tau_F} \tag{10}$$

If relaxation is much slower than the decay of fluorescence, the R-state is not formed, and Eqn. 10 is not applicable. However, if decay and relaxation occur at comparable rates, then $m/\cos \phi$ for the R-state exceeds unity. One expects this to be observable on the red side of the emission. The observation of $m/\cos \phi > 1$ is proof of a time-dependent process. For a single exponential decay $m/\cos \phi = 1$, and for a mixture of fluorophores $m/\cos \phi < 1$ [21].

Estimation of the spectral relaxation time by phase-sensitive detection of fluorescence

Using phase-sensitive detection of fluorescence the emission from any single component can be suppressed by selection of the detector phase angle (ϕ_D). The phase angle for suppression is determined by the lifetime of the fluorophore. This capability is particularly convenient for the analysis of the two-state model described above. Upon examination of the modulated emission with a phase-sensitive detector the phase sensitive intensity is

$$I(\lambda, \phi_D) = \alpha_F m_F I_F^0(\lambda) \cos(\phi_D - \phi_F) + \alpha_R m_R I_R^0(\lambda) \cos(\phi_D - \phi_R). \tag{11}$$

By selecting of the detector phase angle to be 90^0 out of phase with either the F or R state emission the resulting phase-sensitive emission spectrum is representative of the spectral distribution of the unsuppressed emission. Specifically, the emission spectra of the F and R states can be directly recorded by selection of the phase angle of the detector. The emission from the R or F state is suppressed when $\phi_D = \phi_R - 90^0$ or $\phi_D = \phi_F + 90^0$, respectively.

$$I_F(\lambda) = I(\phi_R - 90^0) = \alpha_F m_F I_F^0(\lambda) \sin(\phi_R - \phi_F) \quad (12)$$

$$I_R(\lambda) = I(\phi_F + 90^0) = \alpha_R m_R I_R^0(\lambda) \sin(\phi_R - \phi_F) \quad (13)$$

In our case the phase angles for the F and R states are not precisely known. This is because of spectral overlap and the probability that the relaxation process is more complex than a two-state process. Nonetheless, we used phase suppression on the blue and red sides of the emissions to approximately determine $I_R(\lambda)$ and $I_F(\lambda)$. Conveniently, the F and R state emission are both attenuated by the same factor $\sin(\phi_R - \phi_F)$. The ratio of these phase-sensitive intensities can be used to calculate the spectral relaxation time $\tau_s = k^{-1}$, using Eqns. 1, 2, 12 and 13:

$$\frac{I_F(\lambda)}{I_R(\lambda)} = \frac{m_F}{m_R}\frac{\Gamma}{k} = \frac{m_F}{m_R}\frac{\tau_s}{\tau_0} \quad (14)$$

To calculate τ_s we used the demodulation factors measured on the blue and red sides of the emission as m_F and m_R, respectively. The detector phase angles were those needed to suppress the emission on the blue (400 nm) and red (510 nm) sides of the emission, and τ_0 was the decay time measured through a bandpass filter which transmitted the entire emission spectrum.

Materials and Methods

Synthetic phosphatidylcholines were obtained from Sigma. These were suspended at 8 mg/ml in 0.01 M Tris buffer, containing 0.05 M KCl, pH 7.5, and sonicated to form unilammellar vesicles. Subsequently these were centrifuged ($54\,000 \times g$) for 1 h to remove larger aggregates. Labeling of the lipids was accomplished by mixing the lipid vesicles with TNS dissolved in the same buffer using an initial absorbance of 1.0 at 350 nm, ($\epsilon \simeq 7700\ M^{-1} \cdot cm^{-1}$), and mixing with additional buffer to dilute the lipids to 4 mg/ml, resulting in a lipid-to-probe molar ratio near 100. The lipid vesicles were then incubated for 2 h at 45°C to insure equilibrium of TNS with both sides of the vesicles [23] and to remove structural defects [24]. TNS in glycerol ($A = 0.6$ at 350 nm) was prepared by first dissolving the desired amount of TNS in ethanol or dimethylformamide. The solvent was then evaporated under a stream of argon using gentle heating via a water bath. Following removal of solvent the glycerol was added and the solution stirred slowly for at least 24 h. The high absorbancy of TNS was necessary to make insignificant the background fluorescence from the glycerol.

Fluorescence phase shift and modulation measurements were performed using a modulation frequency of 30 MHz. The excitation wavelength was 340 nm, with an effective bandpass near 2 nm. Apparent phase and modulation lifetimes at various emission wavelengths were measured using interference filters with a bandpass of 10 nm. In addition, all measurements were performed using a Corning 0-52 and a $NaNO_2$ liquid filter, to decrease the intensity of the scattered light. Phase-sensitive spectra were measured with an emission monochromator, as described previously [14,15], with an emission bandpass of 8 nm. All phase angles and demodulation factors were measured relative to the reference fluorophore *p*-bis[2-(5-phenyloxazolyl)]benzene in ethanol with a reference lifetime of 1.35 ns [25]. This procedure minimizes the artifacts which appear when scattered light is used to estimate the phase and modulation of the incident light. These artifacts originate with non-homogeneous modulation of the incident light by the ultrasonic modulator (E. Gratton, personal communication). The effect of Brownian rotation on the measured lifetimes was avoided by using vertically polarized excitation and an emission polarizer oriented 54.7° from the vertical direction [26]. The measured phase angles (ϕ) and demodulation factors (m) were used to calculate the apparent phase (τ_p) and modulation (τ_m) lifetimes using

$$\tan\phi = \omega\tau_p \quad (15)$$

$$m = (1 + \omega^2\tau_m^2)^{-1/2} \quad (16)$$

These apparent lifetimes are convenient because they are more familiar than are the values of ϕ and m.

The rotational correlation times (τ_c) for TNS in glycerol were calculated using the Perrin equation

$$\frac{r_0}{r} = 1 + \tau_0/\tau_c \quad (17)$$

where r_0 is the fluorescence anisotropy in the absence of rotational diffusion, r is the steady-state anisotropy, and τ_0 the fluorescence lifetime. Using our experimental conditions we found $r_0 = 0.357$. These lifetimes (τ_0) and anisotropies (r_0, r) were those observed for the entire emission, as observed through a Corning 4-69 filter.

Results

Fluorescence spectral properties of TNS in glycerol

Interpretation of the data for TNS-labeled vesicles is facilitated by examination of the data for TNS in glycerol. This particular solvent is useful because by variation of temperature its viscosity can be varied over a wide range, thereby varying the rate and extent of solvent relaxation. Steady-state emission spectra measured at various temperatures are shown in Fig. 1. At low temperature (−55°C) the emission maximum is near 410 nm. As the temperature is increased the emission spectrum shifts progressively towards longer wavelength. This shift is essentially complete by 30°C (Fig. 4). Such temperature-dependent spectra are generally attributed to reorganization of the solvent molecules around the increased dipole moment of the excited state. This solvent relaxation is time-dependent, and is expected to alter the fluorescence lifetimes, especially when measured at discrete wavelengths.

Apparent fluorescence lifetimes for TNS in glycerol, measured at various temperatures and emission wavelengths, are shown in Fig. 2. In the presence of time-dependent solvent relaxation the intensity at any given wavelength is not expected to decay exponentially. As a result the phase (τ_p) and modulation (τ_m) lifetimes, calculated from the measured phase angles (ϕ) and demodulation factors (m), are only apparent quantities. At the lowest (< −50°C) and highest (> 25°C) temperatures solvent relaxation is either much slower than emission or complete prior to emission, respectively. Then, the emission is predominantly from a single state and is expected to decay mostly as a single exponential. This was observed at −52°C and +55°C. At these temperatures the phase and modulation lifetimes are essentially identical, and these values are mostly independent of emission wavelength. The residual wavelength-dependence seen at −52°C is probably a result of some solvent relaxation at even this low temperature. In contrast, at intermediate temperatures, −14°C in this case, the apparent lifetimes are strongly dependent upon emission wavelength. Specifically, the apparent phase lifetime increases by 16 ns and the apparent modulation lifetime by 7 ns as the observation wavelength is increased from 380 to 520 nm. The origin of these wavelength-dependent lifetimes can be explained in an intuitive fashion. On the blue side of the emission the apparent lifetime is $\tau_F^{-1} = \Gamma + k$ (Eqn. 4) and is therefore shorter than the lifetime in the absence of relaxation ($\tau_0^{-1} = \Gamma$). This is because the intensity at the shorter wavelengths is decaying by return to the ground state with a rate Γ and by relaxation with a

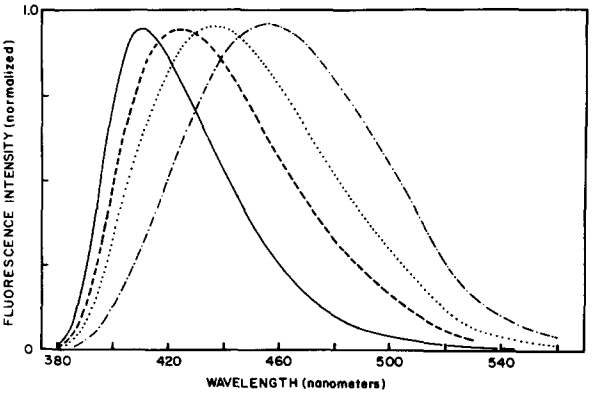

Fig. 1. Fluorescence emission spectra of TNS in glycerol. ———, −55°C; — — —, −20°C; ·····, −5°C; ·–·–·, +25°C.

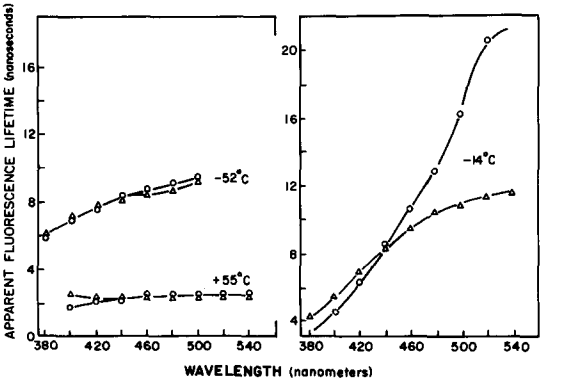

Fig. 2. Apparent phase and modulation lifetimes of TNS in glycerol. O, τ_p; Δ, τ_m.

rate k. At longer wavelengths the apparent lifetime is greater because one is selectively observing those fluorophores which have relaxed prior to emission. These relaxed fluorophores display longer apparent lifetimes because the apparent phase lifetime is given by the sum of the phase angles of the F and the R states (Eqns. 5 and 8). Similar reasoning explains the longer apparent modulation lifetimes at the larger emission wavelengths (Eqn. 7).

The lifetimes seen for TNS in glycerol at $-14°C$ (Fig. 2) are also indicative of the nature of the relaxation process. In particular, both the apparent phase and modulation lifetimes decrease continuously at shorter observation wavelengths. Such results are consistent with the predictions of the continuous relaxation model of Bakhshiev et. al. [17], and with the measurements of Brand and co-workers [9] who used time-resolved measurements and found continous relaxation in glycerol. If the relaxation was a two-state process, and if the spectral separation of states was adequate for selective observation of each state on the edge of the emission, then regions of constant apparent lifetime are expected and observed at the short and long emission wavelengths [20,21]. Evidently, our data are not adequate for an unambigious distinction between continuous and a two-state process. However, we note that in instances where spectral separation is small, the time-resolved method and the phase method are both inadequate to distinguish the continuous and the discrete models.

Conceivably, the wavelength-dependent lifetimes shown in Fig. 2 could be due to the fluorophore being present in two different environments, with the fluorophores emitting at longer wavelengths having the longer lifetime. The two possible origins of wavelength-dependent lifetimes, heterogeneity or an excited state process, can be distinguished by examination of the time-resolved decays of fluorescence intensity. Specifically, a mixture of fluorophores results in a multi-exponential decay with positive preexponential factors. In contrast, an excited state process generally yields a term with a negative preexponential factor [27]. Fortunately, these cases can also be distinguished by phase-modulation fluorometry. This requires measurement of both the phase angle and the demodulation factor. For a multiexponential decay with positive preexponential factors $m/\cos\phi < 1$. For a single exponential decay $m/\cos\phi = 1$, and for a decay with a negative preexponential factor, due of course to an excited state process, $m/\cos\phi > 1$ [20,28]. The values of $m/\cos\phi$ for TNS in glycerol are shown in Fig. 3. At the low and high temperatures $m/\cos\phi$ is approximately equal to unity, independent at the observation wavelength. In contrast, $m/\cos\phi$ is wavelength-dependent at intermediate temperatures, and this value becomes progressively greater than unity as the observation wavelength is increased. The increasing values of $m/\cos\phi$, particularly in excess of 1.0, reflect an increasing contribution of the relaxed state to the total emission at the longer wavelengths. Also, the observation of $m/\cos > 1$ proves that an excited state process, and not ground state heterogeneity, is the origin of the wavelength-dependent lifetimes shown in Fig. 2. With regard to Fig. 2 we note that $m/\cos\phi > 1$ is equivalent to $\tau_p > \tau_m$.

Our temperature-dependent data for TNS in glycerol are summarized in Fig. 4. From these data

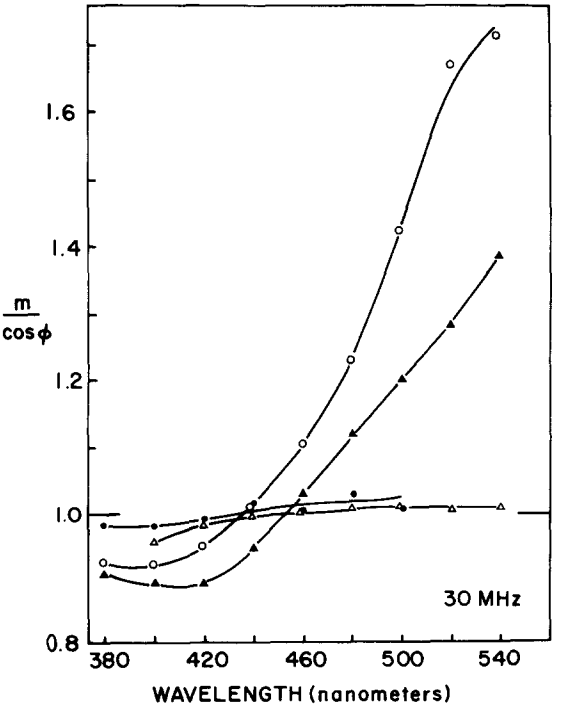

Fig. 3. Wavelength-dependent $m/\cos\phi$ values for TNS in glycerol. ●, $-52°C$; ○, $-14°C$; ▲, $+10°C$; Δ, $+55°C$.

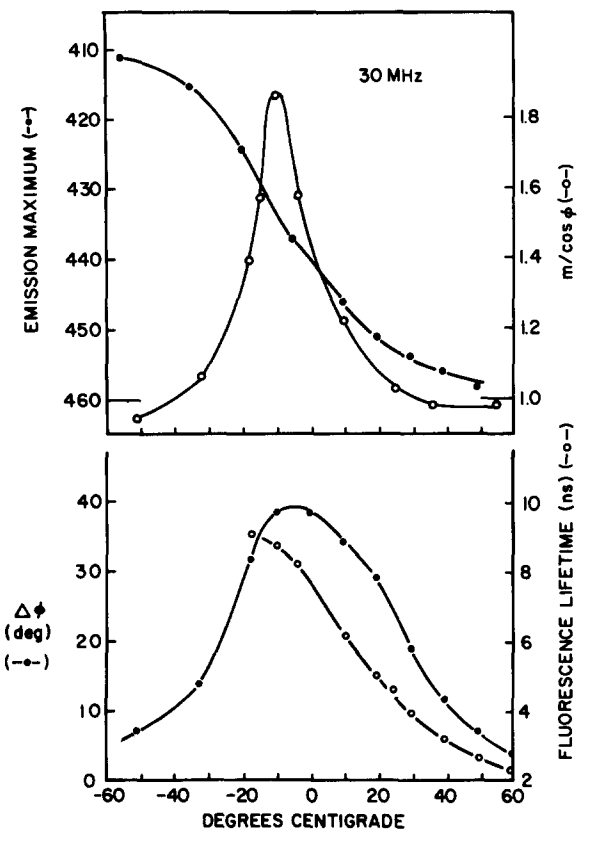

Fig. 4. Effects of temperature on the emission maximum, $m/\cos\phi$ (510 nm), lifetime and $\Delta\phi$ for TNS in glycerol. The lifetime was measured through a Corning 4-69 filter, which passed the entire emission.

it is apparent that the $m/\cos\phi$ values on the red side of the emission exceed unity at those temperatures where the emission maximum is also the most temperature sensitive. The phase difference between the red and blue sides of the emission ($\Delta\phi$) is also maximal near $-10°C$. These data may be regarded as typical of that expected for TNS in an environment for which the relaxation time is comparable to the fluorescence lifetime. Note that values of $m/\cos\phi > 1$ and large values of $\Delta\phi$ are only seen at the intermediate temepratures. At high and low temperatures, when relaxation is either much faster or slower than emission, the spectral properties of the fluorophore are not dependent on emission wavelength. In general, measurements at various temperatures reveal whether the spectral relaxation rate is faster or slower than the decay rate.

The relaxation times for spectral relaxation can be estimated from the phase sensitive fluorescence spectra (Eqn. 14). In this measurement we assume that the emission on the blue and red sides of the emission is dominated by the F and R state emissions, respectively. Then, upon phase suppression at these wavelengths, the phase-sensitive intensities represent the relative intensities of the R and F states. Typical phase-sensitive spectra for TNS in glycerol are shown in Fig. 5. At low temperatures suppression on either side of the emission results in almost complete suppression of the entire emission spectrum. This occurs because at these temperatures the emission is from a single state and the phase angle is nearly constant across the emission spectrum (Fig. 4). Similarly, at high temperature (50°C) suppression of either side of the emis-

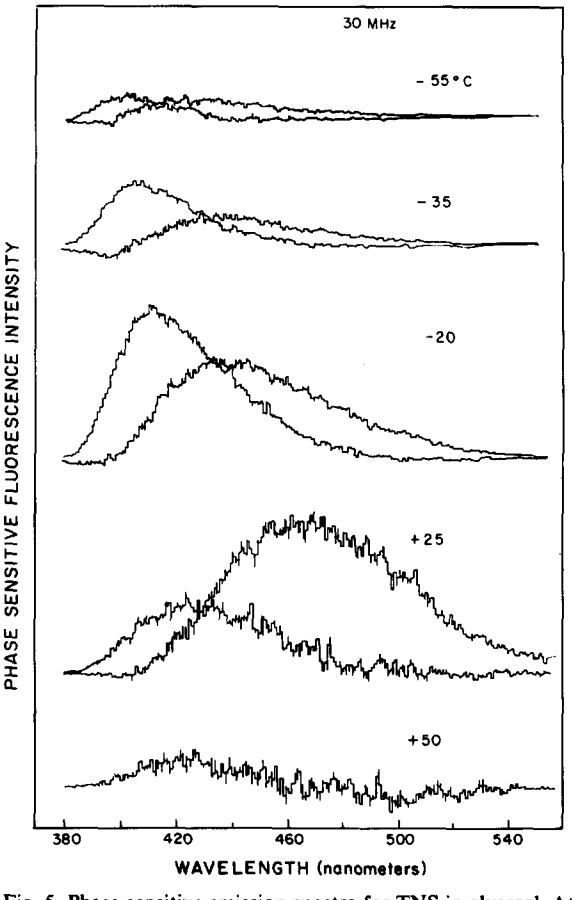

Fig. 5. Phase-sensitive emission spectra for TNS in glycerol. At each temeprature the emission was suppressed on the blue and red sides of the emission. See Table I for more details.

sion also results in suppression of the entire emission. Of course, this is because at 50°C the emission is dominated by that of the relaxed state. Contrasting results are found at intermediate temperatures (−35° to 25°C). Suppression on red and blue sides of the emission results in phase-sensitive spectra which are similar to the steady-state spectra seen at low and high temperatures, respectively (Fig. 1). As the temperature is increased the intensity of the relaxed spectrum is increased, relative to that of the unrelaxed spectrum. We note that the phase-sensitive emission maxima are not independent of temperature. This result indicates that either our simple procedure of red or blue suppression does not result in complete suppression of each state, or more likely, that the simple two-state model is not completely adequate to describe spectral relaxation of TNS in glycerol. Nonetheless, phase suppression does result in an approximated separation of these states.

We used the relative phase-sensitive intensities at each temperature, along with the measured lifetimes and demodulation factors, to calculate the solvent relaxation time (Eq. 14). Some typical values of the measured phase, modulation and lifetime values are listed in Table I. These calculated solvent relaxation times are shown in Fig. 6. Also shown are the rotational correlation times (τ_c) of TNS as calculated from the Perrin equation. Evidently, solvent relaxation occurs more rapidly than rotational diffusion, and with a smaller activation energy (6.4 vs 12.4 kcal/mol, respectively) This disparity is probably a result of the smaller molecular motions needed for spectral relaxation than for rotational diffusion. These results are in agreement with similar data obtained for a tryptophan derivative in a viscous solvent [19]. In total these results indicate that the spectral properties of TNS are highly dependent upon its time-dependent interaction with the solvent. These same spectral properties for TNS, when bound to phospholipid bilayers, should reflect the dynamic properties of these membranes.

TNS-labeled phospholipid vesicles

Representative steady-state spectra of TNS bound to vesicles of dimyristoyl-phosphatidylcholine are shown in Fig. 7. Relative to the emission spectra of TNS in glycerol, only a small temperature-dependent shift was observed. For TNS

TABLE I

PHASE ANGLES AND DEMODULATION FACTORS FOR TNS IN GLYCEROL AND BOUND TO LIPIDS

ϕ_0 is the phase angle measured for the entire emission, using a Corning 4-69 filter. For the lipids the subscripts F and R refer to measurements at 400 and 520 nm, respectively. In the case of glycerol the wavelengths (λ) for measurement were varied with temperature, in order to obtain adequate intensities. Hence λ_F was increased from 395 to 405 nm, and λ_R from 480 to 520 nm, as the temperature was increased from −52°C to +60°C.

Sample	°C	ϕ_F	ϕ_0	ϕ_R	m_F	m_R	I_F/I_R	τ_s (ns)
Glycerol	−32	53.3	59.0	67.9	0.563	0.401	1.50	10.2
	−18	42.2	59.5	73.8	0.651	0.389	1.51	8.4
	−4	36.5	57.1	73.1	0.733	0.460	1.27	6.8
	+10	27.2	50.1	60.8	0.794	0.590	0.72	3.5
	+25	24.7	41.7	45.7	0.807	0.721	0.46	2.0
DMPC	15	38.1	52.1	60.5	0.657	0.543	0.65	4.2
	25	35.1	49.6	59.7	0.703	0.594	0.66	3.8
	35	26.5	45.9	49.0	0.742	0.692	0.56	2.6
DPPC	15	41.5	53.0	57.6	0.589	0.512	0.54	4.1
	25	35.7	51.1	55.0	0.655	0.572	0.48	3.1
	35	33.0	47.8	53.1	0.697	0.599	0.52	2.9
DOPC	15	27.2	45.8	55.0	0.732	0.642	0.55	2.9
	25	25.4	40.3	47.3	0.777	0.683	0.49	2.3
	35	23.6	39.1	41.0	0.802	0.778	0.49	1.7

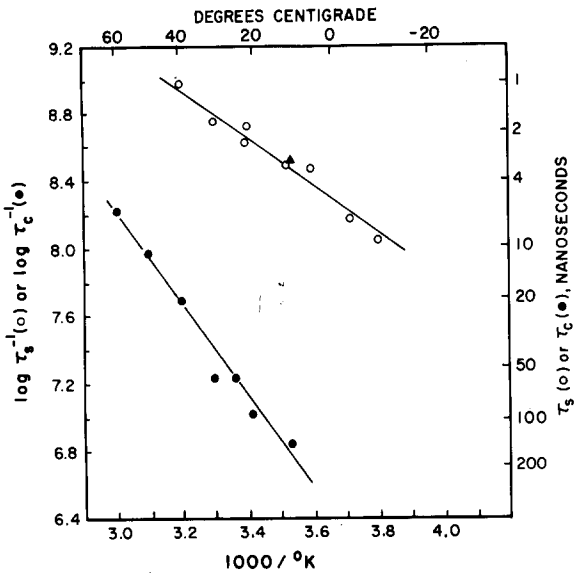

Fig. 6. Arrhenius plot for solvent relaxation ($E_a = 6.4$ kcal/mol) and rotational diffusion ($E_a = 12.4$ kcal/mol) of TNS in glycerol. The triangle (▲) indicates the spectral relaxation time measured by DeToma et. al. [9] using time-resolved emission spectroscopy.

bound to the other lipid vesicles, dioleoyl- or dipalmitoyl-L-α-phosphatidylcholine, the temperature-dependent shifts were comparable or smaller. Such spectra were described previously in greater detail [29]. The small extent of the spectral shifts suggests immediately that the rates of solvent relaxation in bilayers are not strongly dependent upon temperature. We used measurements of the apparent phase and modulation lifetimes, and phase-sensitive emission spectra, to estimate the spectral relaxation rates for TNS bound to lipid bilayers.

Wavelength-dependent phase and modulation lifetimes, and $m/\cos\phi$ values for TNS labeled dimyristoylphosphatidylcholine vesicles, are shown in Fig. 8. As was found for TNS in glycerol at intermediate temperatures, these lifetimes generally increase with increasing wavelength. For these vesicles this effect appears to be maximal near 20°C, which is comparable to the phase transition temperature of dimyristoylphosphatidylcholine, 24°C. The occurrence of an excited state process around the membrane-bound TNS is proven by the observation of $\tau_p > \tau_m (m/\cos\phi > 1)$ on the red side of the emission. At higher temperatures τ_p and τ_m became more comparable in magnitude and $m/\cos\phi \simeq 1$. In addition, the lifetimes became less dependent upon emission wavelength. By comparison and analogy with TNS in glycerol, these results suggests that the spectral relaxation in these membranes is almost complete prior to emission at temperatures above 35°C.

Similar data for vesicles of dioleoylphosphatidylcholine are shown in Fig. 9. These results are similar to those found for the dimyristoylphosphatidylcholine vesicles in that $m/\cos\phi > 1$ on the red side of the emission. However, in contrast with this saturated lipid, the wavelength-dependency of the lifetimes is maximal near 5°C and decreases quickly at higher temperatures. This

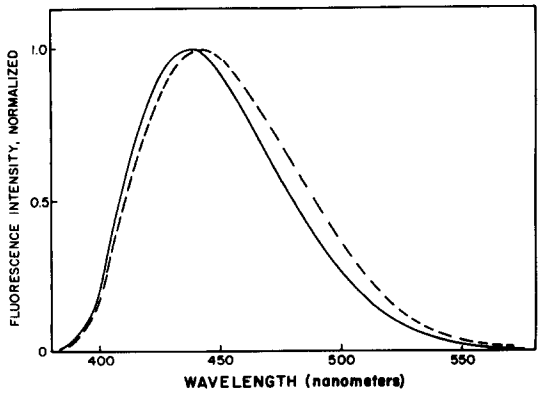

Fig. 7. Emission spectra of TNS-labeled vesicles of dimyristoylphosphatidylcholine. ———, 5°C; — — —, 45°C.

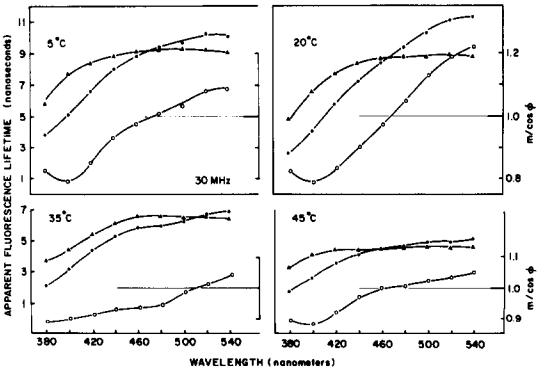

Fig. 8. Wavelength-dependent lifetimes and $m/\cos\phi$ (○) values for TNS-labeled dimyristoylphosphatidylcholine vesicles. ●, τ_p; ▲, τ_m.

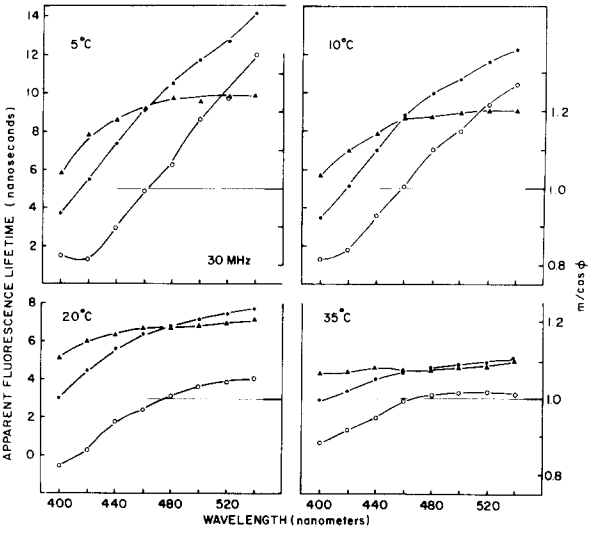

Fig. 9. Wavelength-dependent lifetimes and $m/\cos\phi$ (○) values for TNS-labeled dioleoylphosphatidylcholine vesicles. ▲, τ_p; ●, τ_m.

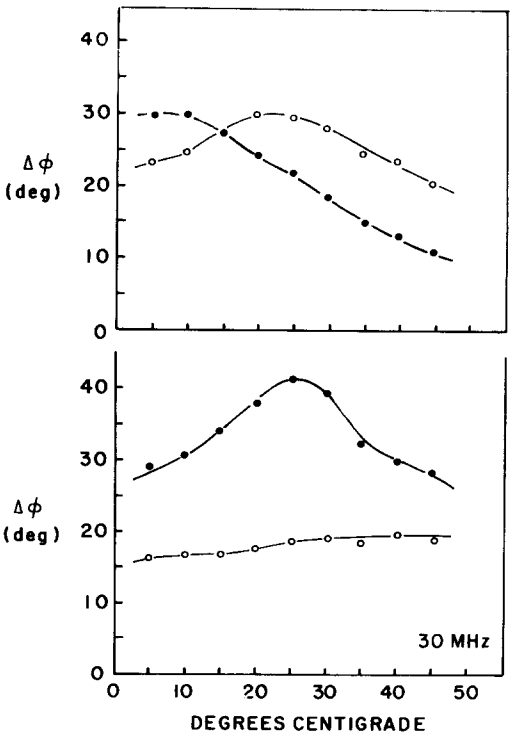

Fig. 10. Phase angle difference ($\Delta\phi$) between the red and blue sides of the emission for TNS-labeled vesicles. The wavelengths use were 380 and 520 nm, except for dipalmitoyl phosphatidylcholine where the wavelengths were 400 and 520 nm. Upper panel: ●, DOPC; ○, DMPC. Lower panel; ●, DMPC/cholesterol (4:1); ○, DPPC.

is expected since dioleoylphosphatidylcholine vesicles are more fluid than vesicles of dimyristoylphosphatidylcholine.

We summarize our wavelength-dependent lifetimes for the labeled vesicles by presenting the phase difference across the emission spectrum (Fig. 10). For dioleoylphosphatidylcholine $\Delta\phi$ decreases progressively with increasing temperature. For both dimyristoylphosphatidylcholine vesicles, with and without incorporated cholesterol, $\Delta\phi$ shows a broad maximum near 25°C. For dipalmitoylphosphatidylcholine $\Delta\phi$ is essentially independent of temperature. Surprisingly, the temperature-dependence of $\Delta\phi$ is rather low for all the lipid vesicles, especially when compared with the $\Delta\phi$ values observed for TNS in glycerol (Fig. 4). Furthermore, the $m/\cos\phi$ values (not shown) measured on the red edge of the emission at 520 nm, are mostly in the range 1.0–1.2, with the values near 1.0 being observed at higher temperatures. These results suggest that the membrane relaxation rates are temperature dependent, but that these rates do not change markedly at the transition temperatures of the lipids.

Phase-sensitive spectra of TNS-labeled dimyristoyl phosphatidylcholine vesicles are shown in Fig. 11. As for TNS in glycerol, the red and blue suppressed spectra are comparable to those expected for the unrelaxed and the relaxed emission of TNS, respectively. However, in contrast to TNS in glycerol, the relative phase-sensitive intensities do not vary widely with temperature, and furthermore, both states are still observable at the lowest (5°C) and highest (45°C) temperatures. These results indicate that at these temepratures the membranes relaxation rates are comparable to the fluorescence lifetime of TNS, and that the ratio of the lifetime to the relaxation time does not vary greatly from 5 to 45°C (Eqn. 14). Also, the phase-sensitive spectral distributions do not vary greatly with temperature. This result should not be taken as evidence for a two-state relaxation of the bilayers around TNS. Rather, the apparent similarity of the phase-sensitive spectra is probably a result of the smaller relaxation-dependent spectral shift of TNS in bilayers as compared with glycerol (Figs. 1 and 7).

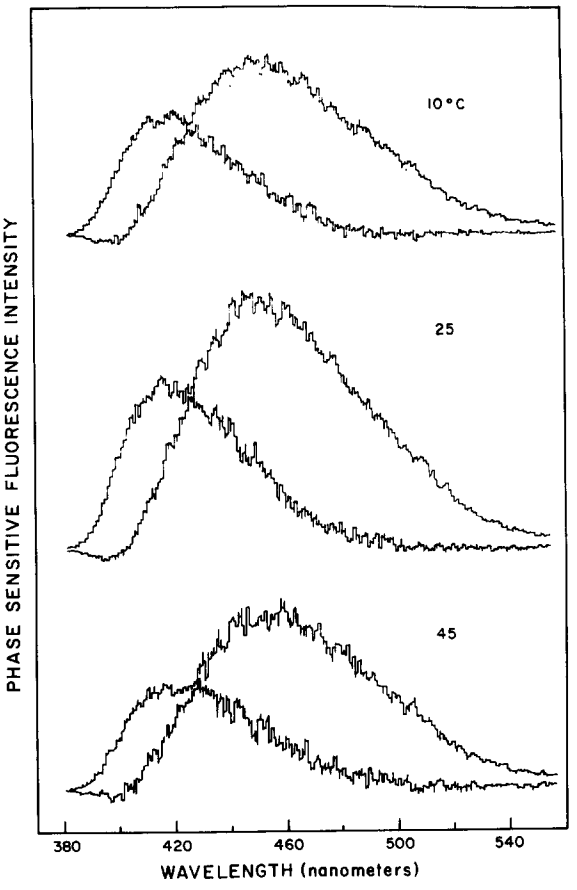

Fig. 11. Phase-Sensitive emission spectra of TNS-labeled dimyristoylphosphatidylcholine vesicles.

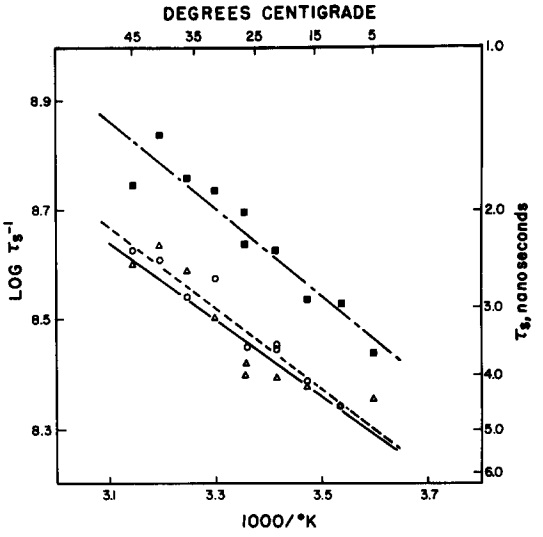

Fig. 12. Arrhenius plot for spectral relaxation of TNS-labeled vesicles, O, TNS in DPPC; ■, TNS in DOPC; △, TNS in DMPC.

Similar phase-sensitive spectra were obtained for TNS-labeled vesicles of dioleoylphosphatidylcholine or dipalmitoylphosphatidylcholine. The relative phase-sensitive intensities and spectral distributions varied only slightly with temperature. These results, along with the measured phase and modulaton values (Table I), were used to calculate the rates of spectral relaxation in these bilayers (Fig. 12). Perhaps suprisingly, but in agreement with previous studies [29], the rates are comparable among the various phosphatidylcholine vesicles. Furthermore, at the lipid-water interface region where TNS is probably localized, the spectral relaxation times are not strongly affected by the phase transition which occurs in the acyl side chain region of these membranes [3]. We conclude that the dynamic properties of the glycerol and polar headgroup region of these phosphatidylcholine vesicles are not subject to the dramatic phase changes found deeper in the bilayer. We note that smaller molecular motions are required for spectral relaxation than for fluorescence depolarization (Fig. 6). The latter process requires displacement of the fluorophore, as well as solvent molecules. Such a distinction was predicted by Bakhshiev and co-workers [31,32].

Our results are in good agreement with other studies of this region of the bilayer using a different methodology. In particular, Shepherd and Buldt [33] determined the dielectric relaxation time of the phosphocholine dipole to be 2.3 ns at 50°C, a value that is close to those we found for spectral relaxation in phospholipids (Fig. 12). As we have seen in the case of DMPC, the polar groups of DPPC show little change in their motion in the presence of cholesterol [34] as determined by NMR. Evidently, the NMR spectral parameters of the polar headgroups of phospholipids are little affected by the composition of the side chains (Ref. 35 and references therein). Also, the activation energy for rotation of the phosphorus in DOPC, as determined by ^{31}P-NMR, is 4.08 kcal/mol [36] which is quite similar to the activation energy for solvent relaxation in this lipid, 3.7

TABLE II

ACTIVATION ENERGIES FOR SPECTRAL RELAXATION OF TNS-LABELED LIPIDS

Lipid	E_a (kcal/mol)
DOPC	3.7
DMPC	3.2
DPPC	3.2
TNS in glycerol	6.4

kcal/mol (Table II). In addition, the correlation time of the phosphate at 5°C (1 ns) is comparable to our spectral relaxation time of DOPC at 5°C (3 ns). However, in the case of DPPE at least, ^{2}H-NMR spectra indicate that the headgroup moves very much faster in the liquid crystalline state than in the gel state [37]. While the broad similarity of our results to these is encouraging, the methods and the phenomena they quantitate may be quite different, and thus the validity of such comparisons is uncertain.

Finally, the results indicate that no large displacement of the phospholipid molecule(s) is necessary to accomplish the relaxation around TNS. The value of the activation energy for relaxation in glycerol (Fig. 6) and the fact that the predominant intermolecular interaction in this solvent is the hydrogen bond suggest that the activation barrier being overcome involves breakage of hydrogen bonds. Similarly, in phospholipids the activation barrier is somewhat lower (Table II), suggesting that fewer and/or weaker hydrogen bonds (or other interactions) must be overcome.

Discussion

In this report we describe the analysis of fluorescence phase shift and demodulation data to reveal the rate of spectral relaxation of a membrane-bound fluorophore. Intuitively, these spectral relaxation rates are revealed most directly by the time-resolved emission spectra. These are the spectra which would be observed at a given instant in time following excitation with a δ-function shaped pulse of light. Rarely are such spectra observed directly, primarily because of the practical limitations of available light sources and detectors. However, time-resolved emission spectra have been computed for TNS in solvents and bound to model membranes [9,10]. These spectra were calculated from the impulse response functions at each emission wavelength. These functions are obtained by analysis the observed decay of emission at each wavelength and the time profile of the pulsed excitation. The excitation pulse width are typically shorter than the decays of intensity. Multi-exponential decays may be determined with reasonable precision, resulting in the ability to determine the time-dependent shift of the emission spectra and hence the spectral relaxation rate. Under favorable circumstances one can determine the time-dependent half-widths of the time-resolved spectra. From these data one can infer whether the relaxation is stepwise or continuous [7,9].

This degree of detail was not available using phase and modulation mesurements at a single modulation frequency. To obtain information equivalent to that described above measurements at a reasonable number of modulation frequencies (about 10) are required. With such data one can determine multi-exponential impulse response functions with good precision, allowing the calculation of time-resolved emission spectra as described above for the pulse fluorometric method. Indeed, this has been accomplished for TNS-labeled vesicles (E. Gratton, J.R. Lakowicz and co-workers, unpublished data) using a newly constructed variable-frequency phase fluorometer. However, the information contained in the single frequency data is simply inadequate to determine the time-resolved spectra. In our estimation, even the use of two or three frequencies, such as are available with commercial instruments, do not allow the time-resolved spectra to be determined. This is because the available data, although formally adequate to resolve a multi-exponential decay, are inadequate to determine the impulse response functions with any reasonable precision. A small error in any of the phase or modulation values will result in substantial errors.

In spite of these limitations it is interesting to indicate the considerable information which is available from the single frequency measurements. There are as follows: 1. The wavelength-dependent phase and modulation lifetimes increased with emission wavelength, indicating the probable ex-

istence of an excited state process (Fig. 2). 2. On the long wavelength side of the emission $\tau_p > \tau_m$ and $m/\cos\phi > 1$ (Figs. 3 and 4). This observation proved the existence of an excited state reaction. 3. Phase-sensitive detection of fluorescence allowed direct recording of the approximate relaxed and unrelaxed emission spectra. 4. Finally, these data allowed the spectral relaxation rates to be calculated. These rates exhibited an Arrhenius temperature dependence, which enabled us to obtain activation energies for this process in glycerol and the bilayers. Thus, it is clear that considerable information can be obtained even from measurements at a single frequency.

Note moreover that the values of the activation energies we obtained seem reasonable when compared with those from other systems. In particular, we found that the values for rotation of and relaxation around TNS in glycerol are somewhat larger (12.4 and 6.4 kcal/mol, respectively) than the corresponding valves for *N*-acetyltryptophanamide in propylene glycol (7.8 and 3.0 kcal/mol, respectively) [19]. Each fluorophore is capable of forming several hydrogen bonds in these suitable solvents, and hence both are likely to behave as isotropic rotors [30]. Being a larger solute in a more polar solvent it is not surprising that larger activation energies are observed in glycerol.

Finally, it is important to relate our results to the most common use of probes such as TNS. There are many studies that attempt to deduce the polarity of a fluorophore-binding site by comparing the spectrum of the bound probe with its spectrum in a particular solvent. As our results and those from other laboratories [10] make clear, caution should be exercised in interpreting such spectra purely in terms of polarity, since it is possible that the binding site may relax at a significantly lower rate than the emission rate of the fluorophore. On the other hand, quantitation of the relaxation offers the prospect of significant dynamic information about the binding site surrounding the fluorophore.

Acknowledgements

This work was supported by Grants PCM 80-41320 and PCM 81-06919 from the National Science Foundation and Grant GM-29318 from the National Institutes of Health. J.R.L. is an Established Investigator of the American Heart Association.

References

1 Singer, S.J. and Nicholson, G.L. (1972) Science 175, 720–731
2 Chapman, D. (1976) Q. Rev. Biophys. 8, 185–239
3 Lentz, B., Barenholz, Y. and Thompson, T.E. (1976) Biochemistry 15, 4521–4528
4 Chen, L.A., Dale, R.E., Roth, S. and Brand, L. (1977) J. Biol. Chem. 252, 2163–2169
5 Kawato, S., Kinosita, K. and Ikegami, A. (1977) Biochemistry 16, 2319–2324
6 Lakowicz, J.R., Prendergast, F.G. and Hogen, D. (1979) Biochemistry 18, 508–519
7 Lakowicz, J.R. (1983) Principles of Fluorescence Spectroscopy, Plenum Publishing Corp., New York, NY
8 Lakowicz, J.R. (1980) J. Biochem. Biophys. Methods 2, 91–119
9 DeToma, R.P., Easter, J.H. and Brand, L. (1976) J. Am. Chem. Soc. 98, 5001–5007
10 Easter, J.H., DeToma, R.P. and Brand, L. (1978) Biochim. Biophys. Acta 508, 27–38
11 Jendrasiak, G.L. and Estep, T.N. (1977) Chem. Phys. Lipids 18, 181–198.
12 Lesslauer, W., Cain, J. and Blasi, J.K. (1971) Biochim. Biophys. Acta 241, 547–566
13 Radda, G.K. (1971) Biochem. J. 122, 385–396
14 Lakowicz, J.R. and Cherek, H. (1981) J. Biochem. Biophys. Methods 5, 19–35
15 Lakowicz, J.R. and Cherek, H. (1981) J. Biol. Chem. 256, 6348–6353
16 MacGregor, R.B. and Weber, G. (1981) Annal. N.Y. Acad. Sci. 366, 140–154
17 Bakhshiev, N.G., Mazurenko, Yu T., and Piterskaya, I.V. (1966) Opt. Spectrosc. 21, 307–309
18 Rapp, W., Klingenberg, H.H. and Lessing, H.E., (1971) Ber. Bunsenges, 75, 883–886
19 Lakowicz, J.R. and Balter, A. (1982) Photochem. Photobiol. 36, 125–132
20 Lakowicz, J.R. and Balter, A. (1982) Biophys. Chem. 16, 99–115
21 Lakowicz, J.R. and Balter, A. (1982) Biophys. Chem. 16, 117–132
22 Spencer, R.D. and Weber, G. (1969) Annal. N.Y. Acad. Sci. 158, 361–376
23 Tsong, T.Y. (1975) Biochemistry 14, 5409–5414
24 Lawaczeck, R., Kainosho, M. and Chan, S.I. (1976) Biochim. Biophys. Acta 443, 313–330
25 Lakowicz, J.R., Cherek, H. and Balter, A. (1981) J. Biochem. Biophys. Methods 5, 131–146
26 Spencer, R.D. and Weber, G. (1970) J. Chem. Phys. 52, 1654–1663
27 Laws, W.R. and Brand, L. (1970) J. Phys. Chem. 83, 795–802

28 Lakowicz, J.R., Cherek, H. and Bevan, R. (1980) J. Biol. Chem. 255, 4403–4406
29 Lakowicz, J.R. and Hogen, D. (1981) Biochemistry 20, 1366–1373
30 Mantulin, W.W. and Weber, G. (1977) J. Chem. Phys. 66, 4092–4099
31 Bakhshiev, N.G. (1966) Opt. Spectrosc. (Engl. transl) 20, 437–441
32 Mazurenko, Y.T. and Bakhshiev, N.G. (1970) Opt. Spectrosc. (Engl. transl.) 28, 490–494
33 Shepherd, J.C.W. and Buldt, G. (1978) Biochim. Biophys. Acta 514, 83–94
34 Brown, M.F. and Seelig, J. (1978) Biochemistry 17, 381–384
35 Seelig, J. and Seelig, A. (1980) Q. Rev. Biophys. 13, 19–61
36 Seelig, J., Tamm, L., Hymel, L. and Fleischer, S. (1981) Biochemistry 20, 3922–3932
37 Blume, A., Rice, D.M., Wittebort, R.J. and Griffin, R.G. (1982) Biochemistry 21, 6220–6230